Pure and Applied Geophysics

Strong Ground Motion Estimation During the Kutch, India Earthquake

R. N. Iyengar[1] and S. T. G. Raghu Kanth[1]

Abstract—In the absence of strong motion records, ground motion during the 26th January, 2001 Kutch, India earthquake, has been estimated by analytical methods. A contour map of peak ground acceleration (PGA) values in the near source region is provided. These results are validated by comparing them with spectral response recorder data and field observations. It is found that very near the epicenter, PGA would have exceeded 0.6 g. A set of three aftershock records have been used as empirical Green's functions to simulate ground acceleration time history and 5% damped response spectrum at Bhuj City. It is found that at Bhuj, PGA would have been 0.31 g–0.37 g. It is demonstrated that source mechanism models can be effectively used to understand spatial variability of large-scale ground movements near urban areas due to the rupture of active faults.

Key words: Strong motion, empirical Green's Function, source mechanism, response spectrum, peak acceleration.

Introduction

The Gujarat earthquake (M_w = 7.7) of 26th January 2001, widely referred to as the Kutch or Bhuj (23.25° N, 69.65° E) earthquake, was a devastating event by any standards. Upwards of 20,000 lives were lost and the earthquake caused direct damage exceeding 5000 million US dollars. As per the Indian Meteorology Department (IMD, 2002), which officially maintains a series of observatories throughout India, the epicenter of this quake was at 23.40°N, 70.28°E. An important feature of this earthquake was the wide-spread liquefaction and ground deformation in the epicentral tracts (Rajendran *et al.*, 2001; Nakata *et al.*, 2001). In nearby places such as Bachau (23.3°N, 70.30°E) and Manfera (23.46°N, 70.38°E) and even in distant locations like Kandla (23°N, 70.1°E) structural damage could be attributed as much to ground failure as to vibratory ground motion. From the engineering point of view, the most sought-after data are strong motion accelerograms (SMA) recorded in the above places. For the present earthquake, the only such instrumental

[1]Department of Civil Engineering, Indian Institute of Science, Bangalore, 560012, India.
E-mail: rni@civil.iisc.ernet.in

record was from the basement of a ten-story building, some 240 kms away from the epicenter, at Ahmedabad (23.04°N, 72.61°E). The other instrumental data available and useful for engineering purposes are on an array of spectral response recorders (SRR) maintained by the Department of EARTHQUAKE ENGINEERING, UNIV. OF ROORKEE (2001). Thus, for this earthquake quantitative estimation of ground motion has to be based on field studies and on analytical approaches. In the present work, near-source ground motion in terms of PGA values is estimated by three different approaches. The results are validated by comparing them with estimates available in the literature (SINGH et al., 2003) and with limited field observations. In the first approach, a source mechanism model based on teleseismic records (MORI, 2001) coupled with a layered half-space regional model is used to simulate displacement time histories in the epicentral region. An empirical relation between PGA and peak ground displacement (PGD) is derived using worldwide data. From this relation the PGA values are obtained from corresponding analytical PGD values. In the second approach, an empirical relation for estimating PGA from SRR data is derived using the global database. This is used to estimate the PGA values at thirteen stations for which SRR values are available. In the third approach, aftershock SMA records are treated as empirical Green's functions (HARTZELL, 1978) to simulate strong motion acceleration time histories at Bhuj by using the method proposed by FRANKEL (1995). From the simulated time histories, an average response spectrum is estimated for the main shock at Bhuj City. Two further estimates of PGA values are obtained from field observation of MMI values and of a few overturned rigid bodies. It is observed that all the methods lead to mutually comparable estimates for the ground motion.

1. Analytical Model

Earthquake mechanisms are complex and the ensuing ground motion at the surface depends on the details of the source, path and site characteristics. The major difficulty in analytical approaches lies in linking the dynamic rupture process occuring at high velocities on fault dimensions of the order of tens of kilometers with surface vibrations that may be of the order of a few centimeters. In this effort, features of the source and path are modeled as for a large primary system and the effect of local topsoil condition is treated as a secondary modification. An earthquake source is described in terms of fault geometry, rupture velocity and slip acting on the fault plane. Similarly, the path is described in terms of geological layers, P- and S-wave velocities, damping factors and densities, some of which may not be known precisely. However, analytical models are expected to handle field data in a broad sense and hence lead to estimates of ground motion in the absence of instrumental records. With these limitations in the background, numerical results are presented here for an eight-layered half-space regional model with a planar rectangular buried fault source (Fig. 1). The regional
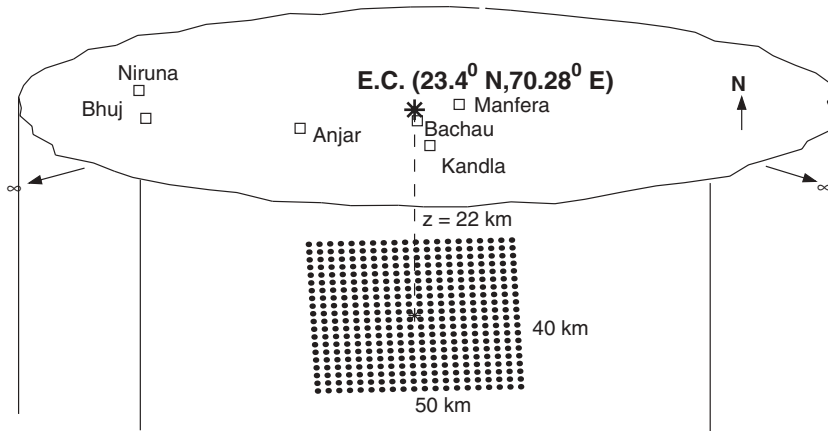
Figure 1
Fault plane and layered half-space regional model.

velocity model used is the one reported by NEGISHI *et al.* (2001). Details of the regional model are presented in Table 1. For the main event source, results of MORI (2001) with constraints on fault geometry from aftershock distribution are used. Accordingly, the rupture size is taken to be 50 km × 40 km with the depth to the top of the fault being 6.7 km. The strike (ϕ) dip (δ) and slip angle (λ) of the fault plane are N 78°E, 45°SE, and 81°, respectively. The rupture velocity is taken as 2.9 km/s. The fault plane is divided into 8000 subfaults of size 0.5 km × 0.5 km, with material rigidity of $\mu = 4.5 \times 10^{10}$ N/m^2. The slip acting on each subfault is represented as a point double-couple varying in time as a ramp function with rise time of 0.13 seconds. The three components of displacements (u, v, w) at a point (x, y, 0) on the surface, for a double-couple source at (0,0,z) are expressed as 3-D Fourier integrals

Table 1

Velocity model for the Kutch region

Depth km.	V_p (km/s)	V_s (km/s)	Density (kg/m^3)	Q_p	Q_S
0–0.2	4.99	2.88	2400	100	50
0.2–0.3	3.40	1.96	2600	100	50
0.3–2.9	4.70	2.72	2900	100	50
2.9–3.0	5.76	3.33	2900	2000	1000
3.0–6.0	6.21	3.59	2900	2000	1000
6.0–20.5	7.01	4.05	2900	2000	1000
20.5–30.0	6.66	3.85	2900	2000	1000
> 30.0	8.47	4.90	2900	2000	1000

$$u(x, y, 0, t) = M_0 \int\limits_{-\infty}^{\infty} \int\limits_{-\infty}^{\infty} \int\limits_{-\infty}^{\infty} \tilde{m}(\omega) \tilde{G}_x(\kappa_x, \kappa_y, \omega, z, \phi, \lambda, \delta)$$

$$\times \, \exp\,(-i\kappa_x x - i\kappa_y y - i\omega\, t)\, d\kappa_x d\kappa_y d\omega$$

$$v(x, y, 0, t) = M_0 \int\limits_{-\infty}^{\infty} \int\limits_{-\infty}^{\infty} \int\limits_{-\infty}^{\infty} \tilde{m}(\omega) \tilde{G}_y(\kappa_x, \kappa_y, \omega, z, \phi, \lambda, \delta) \qquad (1)$$

$$\times \, \exp\,(-i\kappa_x x - i\kappa_y y - i\omega\, t)\, d\kappa_x d\kappa_y d\omega$$

$$w(x, y, 0, t) = M_0 \int\limits_{-\infty}^{\infty} \int\limits_{-\infty}^{\infty} \int\limits_{-\infty}^{\infty} \tilde{m}(\omega) \tilde{G}_z(\kappa_x, \kappa_y, \omega, z, \phi, \lambda, \delta)$$

$$\times \, \exp\,(-i\kappa_x x - i\kappa_y y - i\omega\, t)\, d\kappa_x d\kappa_y d\omega$$

Here (k_x, k_y) stand for the spatial frequencies and ω stands for the temporal frequency. M_0 and $\tilde{m}(\omega)$ and refer to the double-couple magnitude and Fourier transform of the unit ramp function in Haskell's model. $\tilde{G}_x$, $\tilde{G}_y$ and $\tilde{G}_z$ are complex quantities representing the frequency-wave number spectra of the region in terms of P- and S-wave velocities and corresponding damping factors Q_p and Q_s. The derivation of the analytical solution for a layered half-space subjected to point double-couple source has been discussed by BOUCHON (1981) and THEOHARIS and DEODATIS (1994). Hence, further details of the above solution are not presented here. The ground displacement at any station $(x,y,0)$, due to the complete fault rupture, is obtained by summing up the contribution from all the subfaults. Analytical displacement time histories for Bachau and Manfera, which are towns near the epicenter, are shown in Figure 2. In Figure 3, displacement time histories of several other stations, for which SRR data are available, are shown. The displacement field has been computed on a grid size of 1 sq km covering a region of dimension 200 km × 200 km. In Figures 4 a,b,c permanent surface displacements in the eastwest, northsouth and vertical directions are presented. It is known that displacements are controlled by long-period components, whereas accelerations are sensitive to high frequencies. In the present work, it has not been possible to include frequencies beyond 2 Hz. However, this limitation is circumvented by adopting an empirical approach to relate computed peak displacements with PGA values.

PGD-PGA Relationship

Here, a simple new approach is developed which connects the analytical peak ground displacements of the previous section with PGA values. For this purpose global strong motion data are collected from the websites of Pacific Earthquake Engineering Research Center (*http://peer.berkeley.edu/*) and COSMOS (http://*cosmos-*
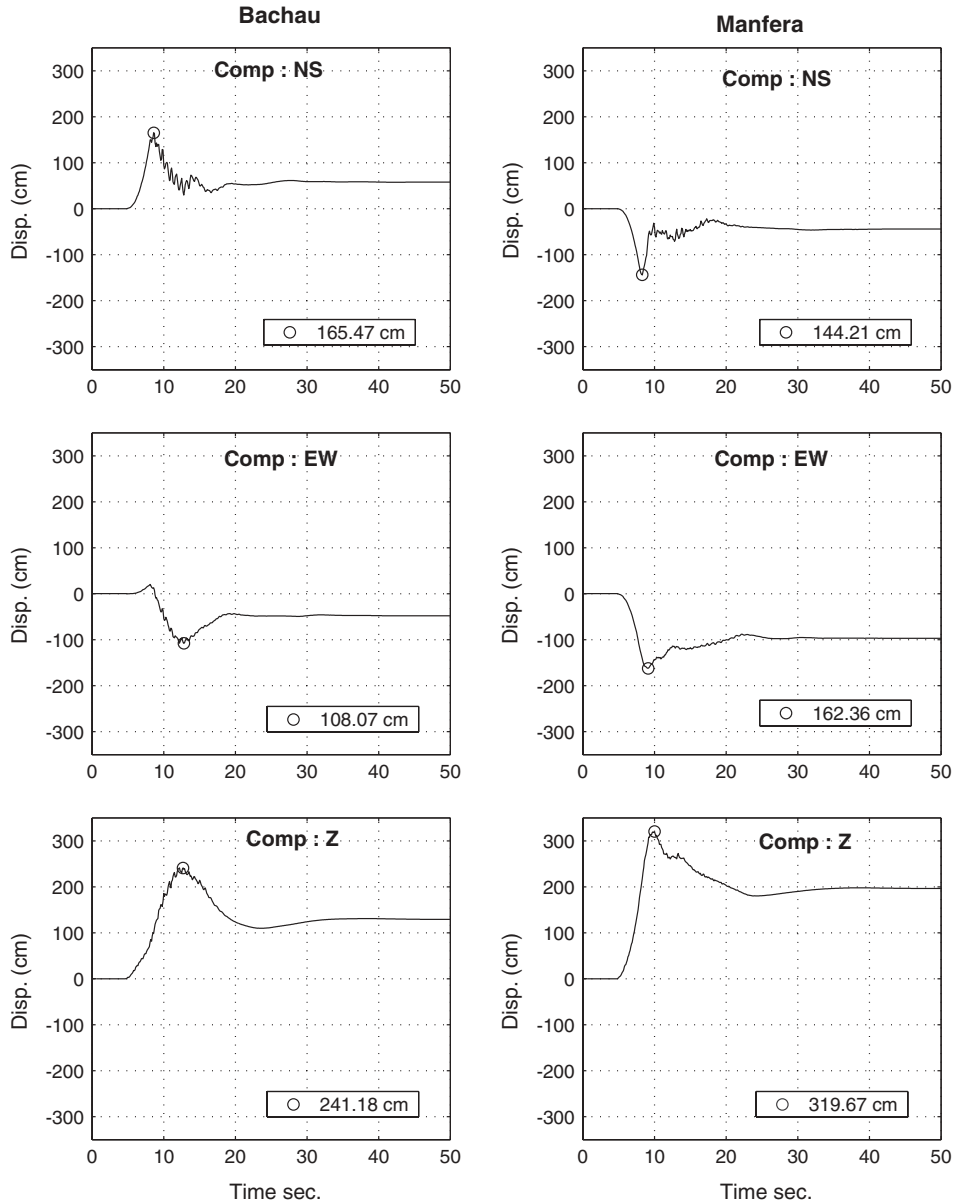
Figure 2
Analytical surface displacement time histories (Cm.) at Bachau and Manfera o - Peak value.

eq.org). Ninety-four PGA and PGD values are selected corresponding to NEHRP-A site condition (Bssc, 2001). A linear regression between ln (PGA) and ln (PGD) of the type,
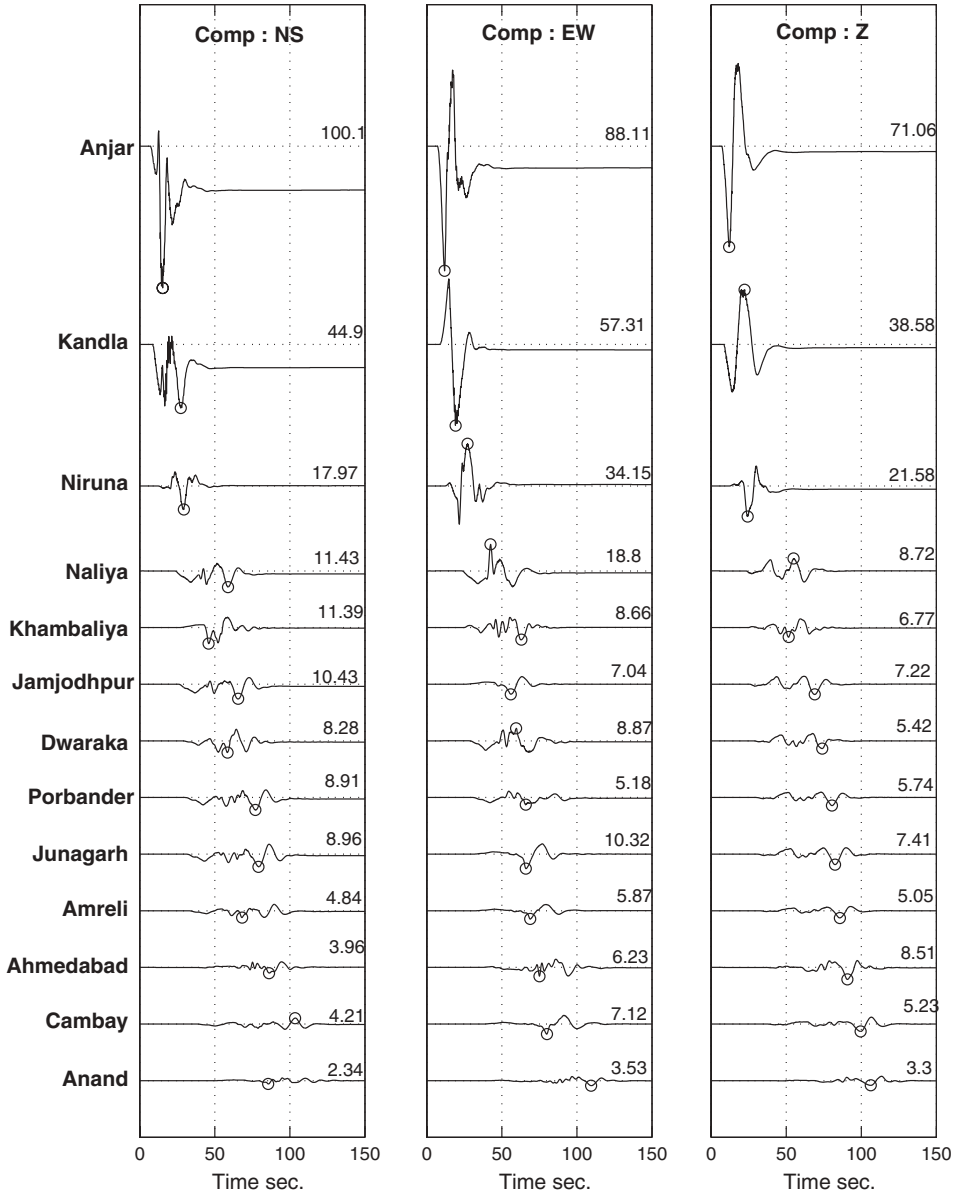
Figure 3

Analytical surface displacement time histories (Cm.). o - Peak value.

$$\ln{(\text{PGA}/g)} = 0.74 \ln{(\text{PGD})} - 4.493; \sigma(\varepsilon) = 0.41 \tag{2}$$

is developed as shown in Figure 5. This relationship can be used for estimating PGA from analytically simulated PGD values. It is noted here that the recorded
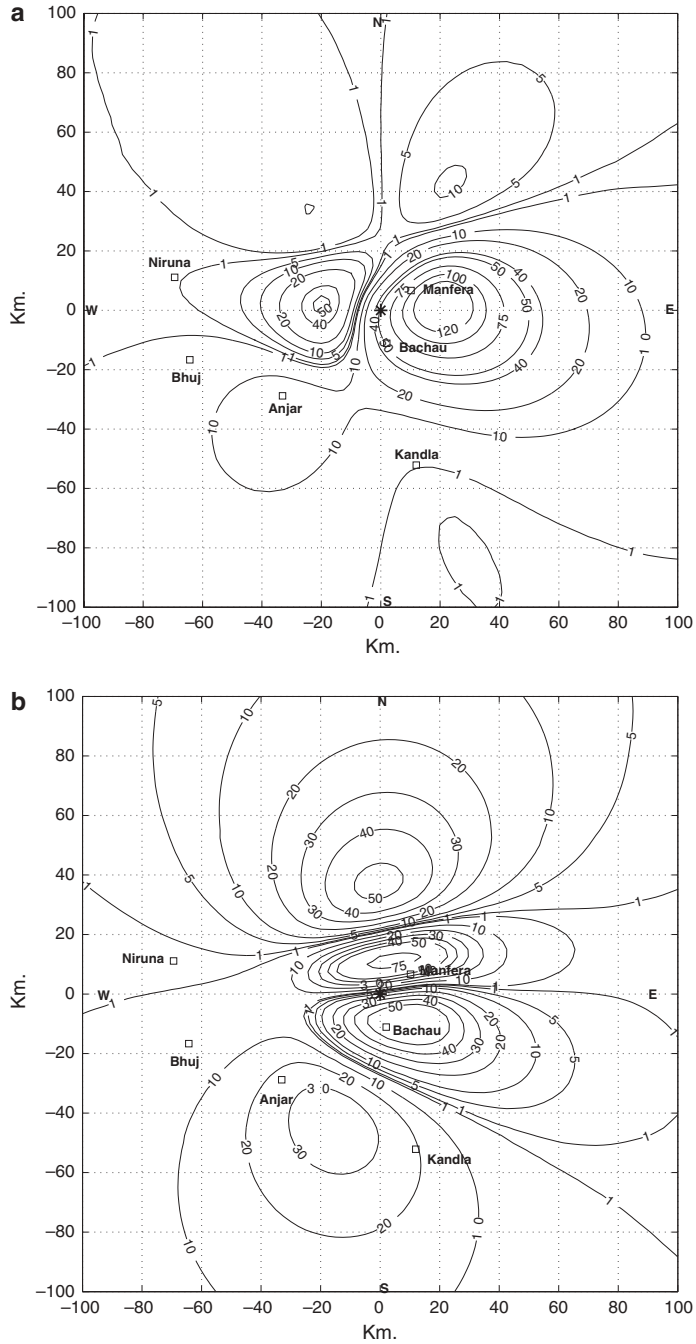
Figure 4
a Permanent surface displacement (Cm). A-type site. E-W component. b Permanent surface displacement
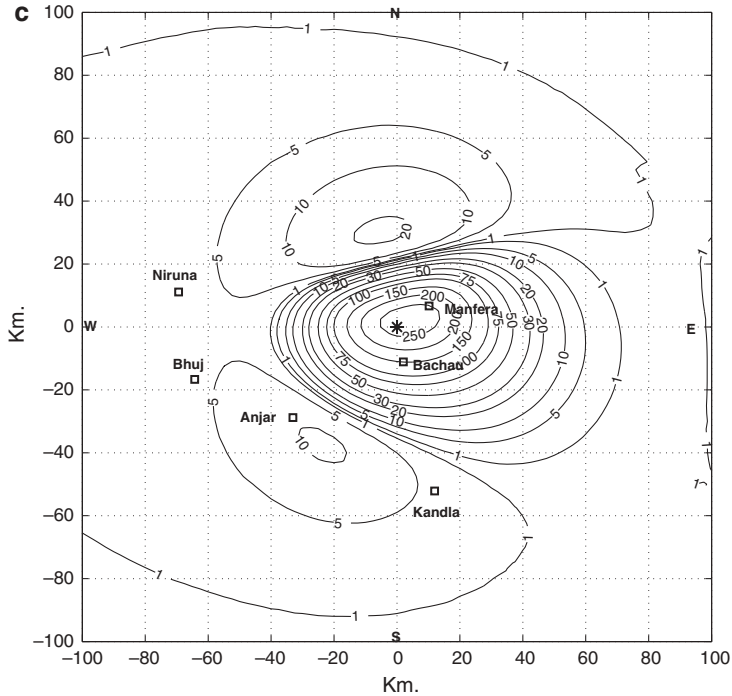(Cm.). A-type Site. N-S component.

Figure 4c
Permanent surface displacement (Cm). A-type site. Vertical component.

global data have been filtered below 0.07 Hz to remove long-period trends. Hence, the computed displacement time histories are also high passed in the same frequency range before PGD values are converted to PGA values. Contours of resultant horizontal PGA in the Kutch region corresponding to A-type soil, estimated in this fashion are shown in Figure 6. These contours indicate high PGA in the northeast direction from the epicenter around Bachau. This is consistent with the observations of HISADA and MEGURO (2001) based on isoseismal patterns. Before the present results can be compared with instrumental results, it would be interesting to compare them with the theoretical results of SINGH et al. (2003). These authors have used an improved version of the one-dimensional stochastic simulation model of BOORE (1983), proposed by BERESNEV and ATKINSON (1997), to arrive at expected PGA values at thirteen stations with SRR data. A comparison between the present results with those of SINGH et al. (2003) is presented in Table 2. The present values are valid for NEHRP-A condition whereas the results of SINGH et al. (2003) are for bedrock condition with V_s = 3.6 km/s. Hence, the present PGA values are greater than the estimates of SINGH et al. (2003), which is to be expected.
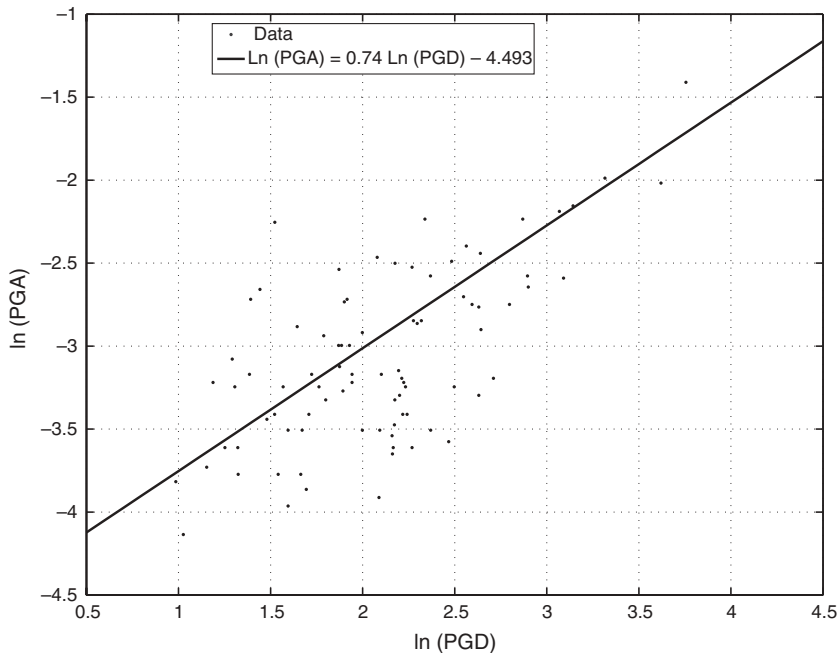
Figure 5
PGA-PGD relationship derived from global data.

Estimation of PGA from SRR Data

In the absence of recorded strong motion accelerograms one must validate the analytical results indirectly using spectral response recorder data. These instruments give a trace of the response of a laterally oscillating tuned single degree-of-freedom system, with a known damping coefficient η and natural period. In the Kutch region, four sets of instruments with $\eta = 0.05$; 0.1 and $T_n = 0.4$; 0.75 seconds were operating at thirteen stations. Thus, the spectral acceleration $S_a(\eta, T_n)$ at these stations could be read directly from such records. Since S_a is correlated with PGA, the latter can be indirectly estimated with the help of SRR data. With this in view, an empirical equation connecting the above S_a values with PGA has been previously derived by IYENGAR and RAGHUKANTH (2004). The regression equation is of the form

$$\ln(\text{PGA}) = a_1 + a_2 \ln[S_a(0.05, 0.4)] + a_3 \ln[S_a(0.05, 0.75)] + a_4 \ln[S_a(0.1, 0.4)] \\ + a_5 \ln[S_a(0.1, 0.75)] + \ln \delta \tag{3}$$

$$a_1 = -0.5158; \ a_2 = 0.25; \ a_3 = -0.2488; \ a_4 = 0.8586; \ a_5 = 0.2922; \ (\sigma \ln \delta) = 0.3429. \tag{4}$$
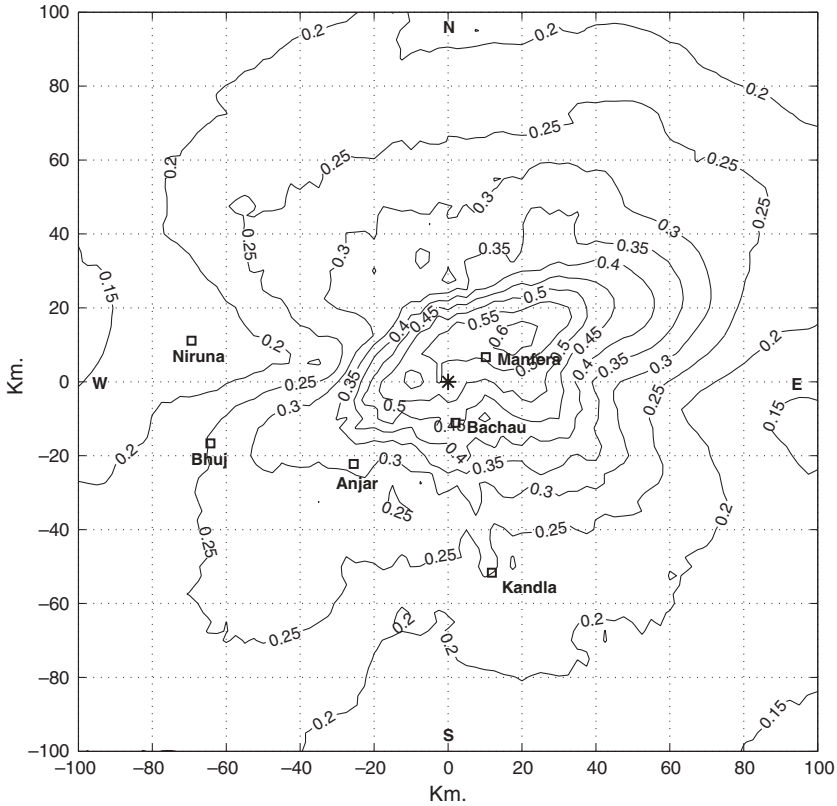
Figure 6
Analytical estimate of horizontal peak ground acceleration. A-type site.

PGA values so obtained are still estimates with some scatter but are valid for local site conditions. On the other hand, the analytical PGA estimates are valid for A-type site conditions. Hence, these analytical values are to be corrected for local site conditions before a comparison becomes meaningful. This has been previously pointed out by CRAMER and KUMAR (2003) who also converted SRR values into PGA results, depending on the site conditions. In Table 3, PGA values estimated from the above equation are presented along with analytical estimates, corrected for site conditions as per the NEHRP provisions (BSSC, 2001).

Empirical Green's Function (EGF)

The methods presented above give an estimation of PGA during the earthquake. However, peak values alone do not provide complete representation of ground motion. Several other characteristics such as frequency content and duration are

Table 2

Comparison between analytical results of SINGH et al. and authors

Station	Epicentral Distance (km)	SINGH et al. PGA-g Vs = 3.6 km/s	Authors PGA-g Vs = 2.88 km/s
Anjar	44	0.254	0.342
Kandla	53	0.285	0.236
Niruna	97	0.101	0.162
Naliya	147	0.067	0.104
Khambaliya	150	0.069	0.070
Jamjodhpur	166	0.053	0.066
Dwaraka	188	0.049	0.057
Porbander	206	0.037	0.053
Junagarh	216	0.032	0.067
Amreli	225	0.031	0.049
Ahmedabad	238	0.029	0.049
Cambay	266	0.022	0.053
Anand	288	0.021	0.036

equally important in practical problems. In engineering practice, acceleration time history is the most sought-after information. But as noted earlier, analytical methods have limitations in correctly simulating the frequency structure of acceleration time histories. In addition, the isotropic horizontally layered Earth model is an idealization of a very complex medium with uncertain properties. Nevertheless,

Table 3

Comparison among PGA estimates

Station	Site Condi-tion	MMI	$\eta = 0.05$		$\eta = 0.1$		SRR-PGA (Eq. 3,4)	PGD-PGA Modified for site condn.	MMI-PGA (Eq. 9)
			T = 0.4 s SRR Sa(g)	T = 0.75 s SRR Sa(g)	T = 0.4 s SRR Sa(g)	T = 0.75 s SRR Sa(g)			
Anjar	C	IX	1.62	0.70	0.91	0.69	0.62	0.513	0.49
Kandla	C	VIII-IX	0.86	0.57	0.65	0.53	0.41	0.354	0.35
Niruna	D	VIII-IX	0.81	0.65	0.76	0.55	0.44	0.324	0.35
Naliya	C	VIII	0.72	0.22	0.69	0.21	0.40	0.156	0.25
Khambaliya	A	VI-VII	0.18	0.07	0.09	0.04	0.06	0.070	0.09
Jamjodhpur	A	VI-VII	0.22	0.15	0.14	0.05	0.07	0.066	0.09
Dwaraka	D	VI-VII	0.21	*	0.18	0.11	0.11	0.114	0.09
Porbander	D	VII	0.19	0.25	0.15	0.21	0.10	0.106	0.13
Junagarh	A	VI	0.19	0.06	0.10	0.05	0.07	0.067	0.06
Amreli	A	VI	0.09	0.07	0.07	0.05	0.05	0.049	0.06
Ahmedabad	D	VII-VIII	0.29	0.23	0.24	0.19	0.15	0.098	0.17
Cambay	D	VI	0.49	0.04	0.29	0.04	0.19	0.106	0.06
Anand	D	VI	0.14	0.06	0.12	0.05	0.08	0.072	0.06
Bhuj	B	IX	–	–	–	–	–	0.310	0.49

within the scope of linear system theory, Green's function or impulse response function holds the key to the final solution. This function is the surface level response of the region under consideration to a buried impulsive double-couple applied at an arbitrary point. Thus, small magnitude earthquakes with point-like sources should directly provide a clue to the regional Green's function. In practice, since a point source is an idealization, suitable scaling is necessary in estimating EGF. HARTZELL (1978) proposed that records of small magnitude earthquakes occurring near the main shock fault plane could be taken as EGF in simulating the ground motion for the target region. In recent years, two broad EGF approaches are in vogue. In the first approach, the main shock fault plane is divided into sub-faults of equal size. The number of such subfaults is determined from the scaling law of KANAMORI and ANDERSON (1975). Each subfault is taken to produce the recorded accelerogram of the aftershock or small magnitude event, with a correction factor (FRANKEL 1995). Each such accelerogram is delayed at the surface station to account for rupture time and travel time from the various subfaults that make up the main fault. In the second approach, the EGF is obtained by deconvolution of the aftershock record (HUTCHINGS, 1994; ARCHULETA et al., 2003). The possible main shock fault plane is divided into a large number of subfaults and the contributory ground motion of each subfault is obtained by convolving the estimated EGF with a prescribed source time function. In this approach a greater number of parameters are required, which may not be precisely known. In the context of the Kutch earthquake, strong motion data of three aftershocks, recorded at Bhuj observatory, are available. Here, the approach of FRANKEL (1995) requiring a single Green's function is adopted. The main shock fault plane, as reported by MORI (2001), is divided into subfaults of area,

$$A_s = \left(\frac{M_s}{M_m}\right)^{\frac{2}{3}} A_m. \tag{5}$$

Here M_m and M_s are the moment values of the main event and aftershock, respectively. A_m is the area of the main shock fault plane taken to be rectangular. Following FRANKEL (1995), the ground acceleration at Bhuj during the main event can be expressed as a sum of N convolutions to obtain

$$\ddot{U}_m(t) = \sum_{i=1}^{N} C_i\left(\frac{R}{R_i}\right)[S(t) * \ddot{u}(t - t_{si} - t_{ri})]. \tag{6}$$

Here $\ddot{u}(t)$ is the recorded acceleration (EGF) corresponding to subfault i. C_i is the ratio of the stress drop in the i-th fault to that of the small aftershock event. R_i is the distance of the i-th fault to the surface station and R is the hypocentral distance between the station and the source of the aftershock. The shear-wave travel time t_{si} from i-th fault to the station can be computed from the velocity model (Table 1). The EGF is further delayed by the rupture time t_{ri}, found as the ratio of the distance between the i-th fault and the main shock hypocenter, to rupture velocity. The stress drop ratio C_i is taken as (PITARKA et al., 2000)

$$C_i = \left[\frac{(A_m/A_s)}{\sum_{i=1}^{N}(d_i/d_{max})^2}\right]^{\frac{1}{2}}\frac{d_i}{d_{max}}, \tag{7}$$

where d_i is the slip on the i-th fault and d_{max} is the maximum slip. The Fourier transform of the source time function $S(t)$ is of the form (FRANKEL, 1995)

$$S(f) = \left(\frac{M_m}{\sum_{i=1}^{N}C_iM_s}\right)\left[\frac{1+(f/f_s)^2}{1+(f/f_m)^2}\right], \tag{8}$$

where, f_s is the corner frequency of the aftershock records. The corner frequency of the main event record is taken as $f_m = f_s/[\sqrt{(M_m/\sum C_iM_s)}]$. The details of the three aftershocks, used here as EGF, are given in Table 4. The acceleration records of the three aftershocks are shown in Figure 7. The fault geometry is the same as that used in the analytical model (Fig. 1). Other data required for the main event are taken from the results of MORI (2001). Three sample simulated acceleration time histories for Bhuj City during the main shock are shown in Figure 8. These correspond to the three aftershock records as starting EGF. In Figure 9, the response spectra of the six horizontal components along with their average are presented. Random variations persist in the samples, attributable to differences in stress drop and path effects of different EGF. This method estimates the main shock PGA at Bhuj City to have been between 0.33 g–0.37 g. This value matches well with estimates from other approaches. The response spectra so obtained for Bhuj show high frequency content consistent for hard rock. It may be noted here that Bhuj observatory, where the aftershock SMA were obtained, is on hard rock.

PGA from Field Investigation

The above analysis has confined itself to finding PGA values from theoretical approaches, combined with empirical results, valid in a global sense. It would be interesting to see how well the above results correlate with field observation of damage after the earthquake. MMI values are primarily assessments of the observed effect of ground motion on manmade structures. Thus, a reasonable correlation

Table 4

Parameters of main shock and aftershocks

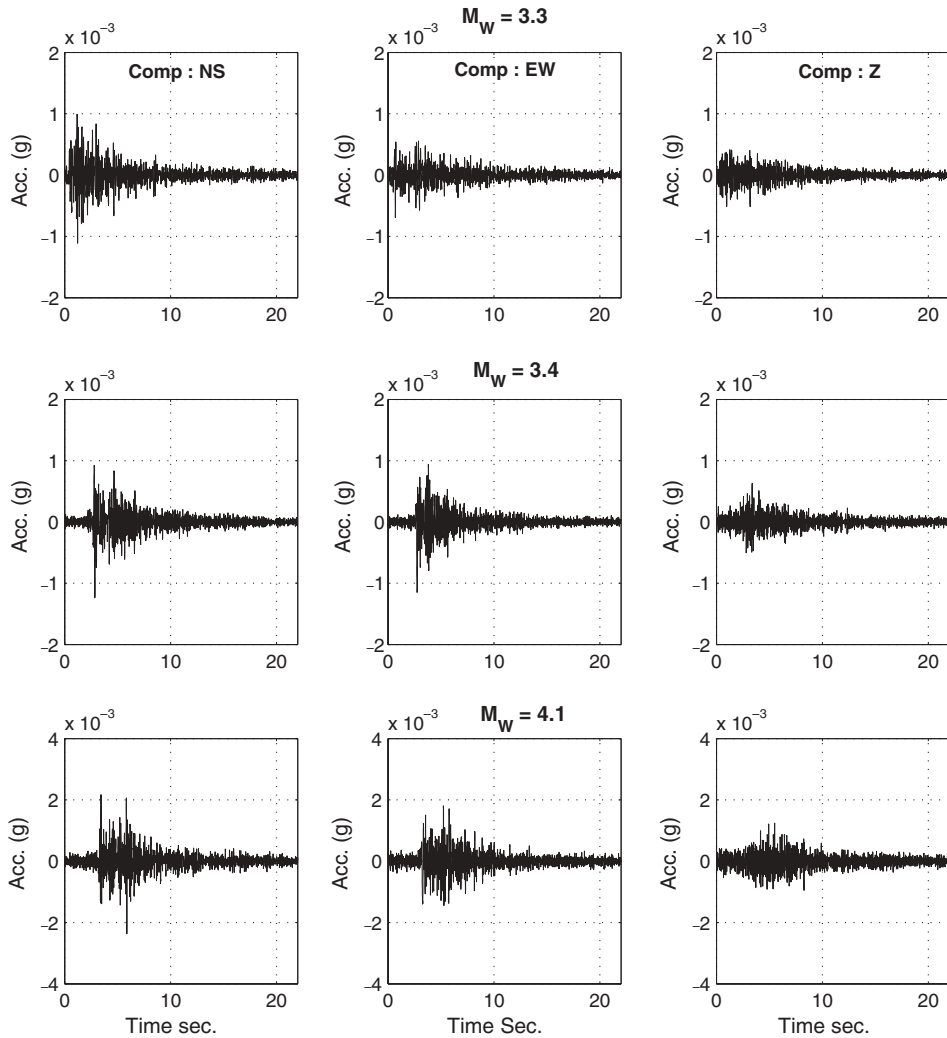| Date	Magnitude (M$_w$)	Epicenter		Focal Depth (km)	Corner Frequency (Hz)	Number of Subfaults N
26 / 1 / 2001	7.7	23.40°N	70.28°E	22	–	1
6 / 2 / 2001	4.1	23.38°N	70.38°E	15	5.2	2929
7 / 2 / 2001	3.4	23.49°N	70.32°E	15	7.1	14678
7 / 2 / 2001	3.3	23.29°N	70.34°E	15	7.3	18478

Figure 7
Aftershock acceleration time histories at Bhuj Observatory (23.25°N, 69.65°E).

between MMI and PGA values can be expected. However, it has to be recognized that the damage pattern and level depend on the vulnerability of the structures, which in turn varies from country to country. Hence MMI-PGA relation would be strongly country specific. Hence, for estimating PGA from MMI values of the Kutch earthquake, relations developed for other parts of the world (WALD et al., 1999; TRIFUNAC and BRADY, 1975; AMBRASEYS, 1974) will not be applicable. In the Indian context, construction practices may be taken to be similar throughout the country, except for differences in material composition in rural areas. Previously the present
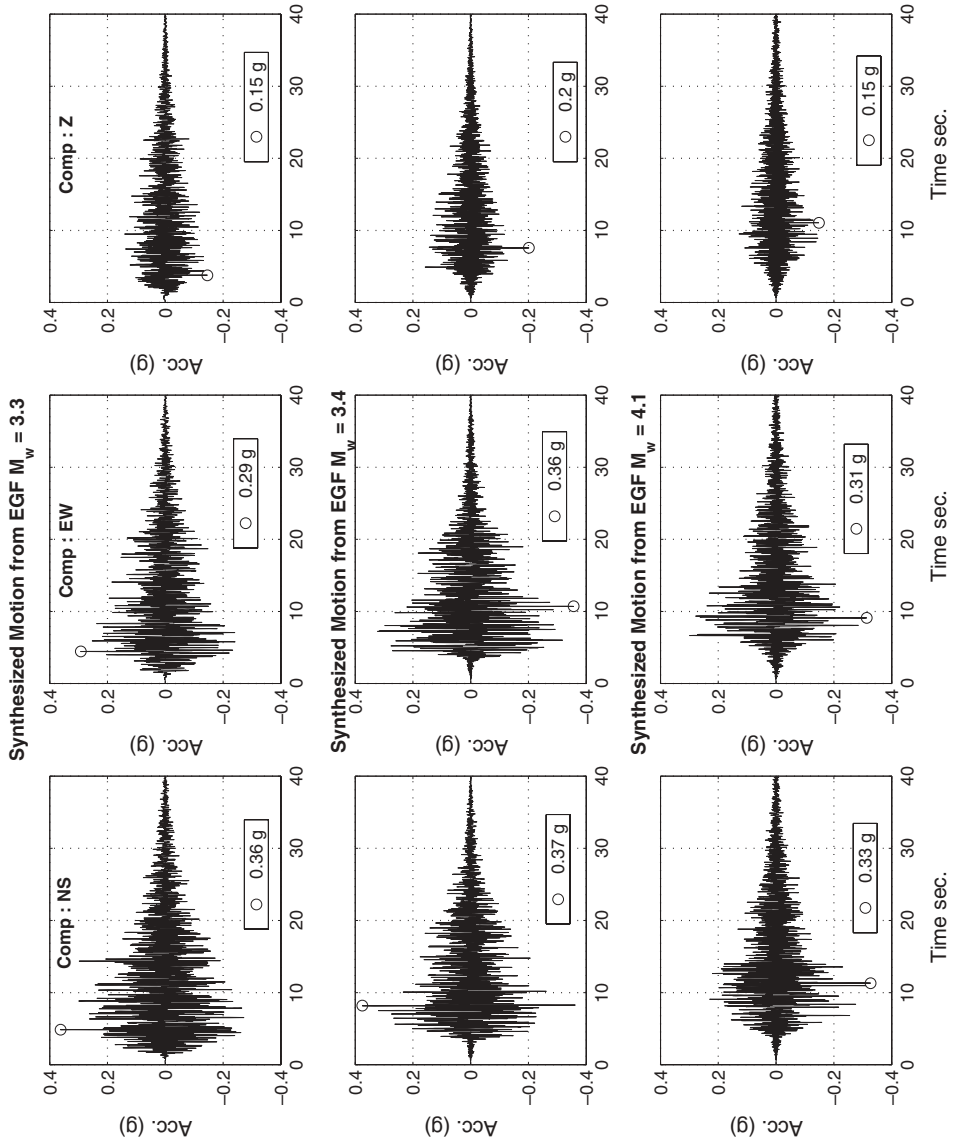
Figure 8
Simulated accelerograms for the main event of 26th January, 2001 at Bhuj City based on EGF.

authors (IYENGAR and RAGHUKANTH, 2003) addressed this question of relating Indian MMI data with instrumental PGA data with the aid of forty-three sample values. A linear regression between ln(PGA) and MMI leads to

$$\ln (PGA/g) = 0.6782 \, MMI - 6.8163; \, \sigma(\ln \varepsilon) = 0.731. \qquad (9)$$
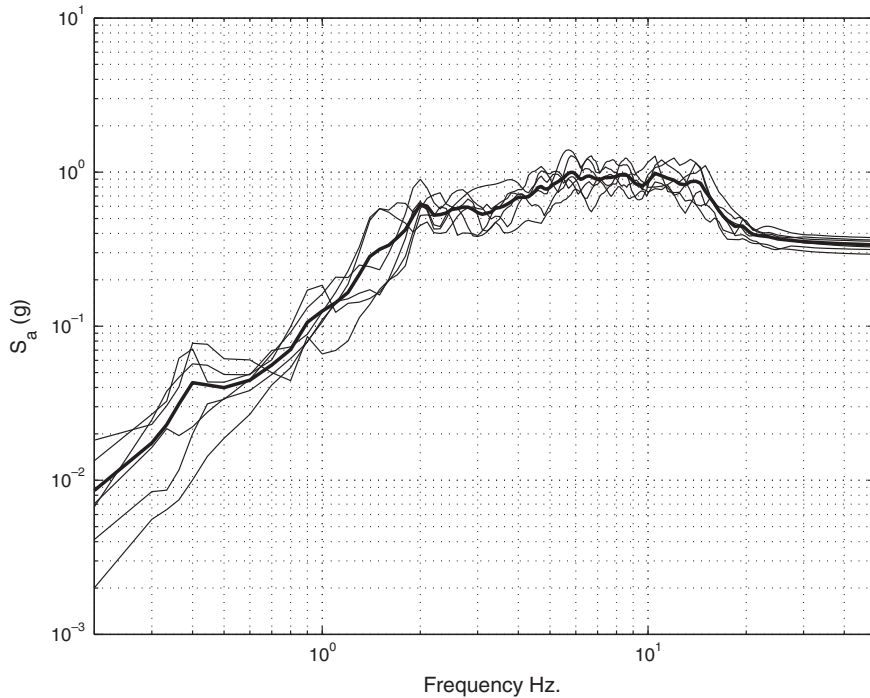
Figure 9
Sample and mean response spectrum in horizontal direction at Bhuj City ($\eta = 0.05$).

A comparison of this result with other such equations shows for a given value of MMI, the present equation predicts a lower value of PGA than others. This may be interpreted as a reflection of the higher vulnerability of the Indian built environment, as compared to the Californian or the European habitat, at the same level of hazard. Equation (9) is a relation for the expected PGA values only. In practice PGA will be distributed as a random variable and hence recorded values will show considerable variation in a region with nearly constant MMI. In the present study MMI estimates as reported by HISADA and MEGURO (2001) are used in finding PGA values from Equation (9) at some stations. These are compared in Table 3 with the corresponding PGA values as given by SRR instrumental data. There is a possibility of estimating PGA values in the field from observing overturned rigid bodies such as concrete pillars, gravestones and storage racks. This approach has been previously adopted by IYENGAR et al. (1994) in the field investigation of the Khillari earthquake. For the Kutch earthquake also, IYENGAR et al. (2001) have collected information on a set of about 20 rectangular rigid objects that had overturned or rotated about their base during the earthquake. Two typical objects that reliably rocked about their base are shown in Figures 10 and 11. The minimum ground acceleration needed to lift such an object is the ratio (b/h), where b is half the base width and h is the height of the body

Figure 10
Overturned object at Adhoi (23.4°N, 70.5°E). (b/h) = 0.61.

centroid from the base. PGA values estimated from various methods are plotted in Figure 12, with respect to epicentral distance to understand the attenuation of PGA of the main event.

Discussion

The non availability of SMA records for the Bhuj earthquake, motivates one to search for alternate means of estimating PGA values in the epicentral region. Here, it is found that source mechanism models based on teleseismic data can be effectively used to arrive at displacement time histories. The permanent displacement contours shown in Figures 4a,b,c are valid for an ideal linear elastic system, with the stated properties. In reality the near surface soil would behave in a nonlinear fashion with the permanent displacements becoming readjusted within a few days or weeks to different levels. Hence, large displacements in the linear model would hint at ground failures due to a high level of strains. Places like Bachau and Manfera that indicate large displacements of the order of a few meters are likely candidates for ground cracks and openings which has been verified to be true from field investigations. Thus the results of Figures 4a,b,c are largely indicative of the relative variation of foundation level distress for the built environment. Although, theoretically surface acceleration can also be computed by such methods, computational difficulties put limits on the high frequency end of the spectrum. To circumvent this difficulty, here the PGD estimates are converted to PGA values empirically to arrive at Figure 6. The shape of this figure correlates well with known MMI variation for this

Figure 11
Overturned object at Kandla (23°N, 70.1°E). (b/h) = 0.31.

earthquake. Also this figure brings out the directivity effects due to fault orientation and slip direction. It is observed that PGA values are higher in the NE direction of the epicenter. For comparable epicentral distances PGA values are higher to the east of the epicenter than to the west. This figure also highlights the non-axisymmetric nature of PGA distribution during a strong earthquake. The estimated PGA values are useful in understanding how ground motion attenuated with distance. The present results are validated with the help of SRR data and an alternative analytical simulation carried out by SINGH et al. (2003). The comparisons at specific stations are shown in Tables 2 and 3. It is seen that the present figures compare well with the other two sets of results. Stations such as Naliya where the differences are large, have soft soils leading to local effects. The layered regional model is not tuned to handle such effects yet. The EGF based simualtion has been possible for only Bhuj City. The
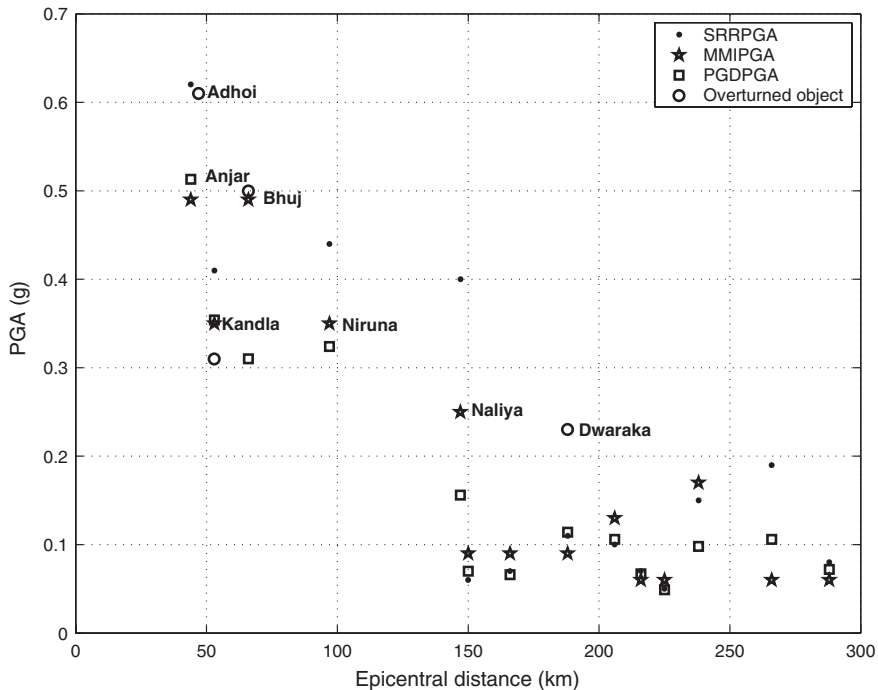
Figure 12
Attenuation of PGA during the main event ($M_w = 7.7$).

simulated samples show PGA in the range of 0.33 g–0.37 g, which matches with other estimates for Bhuj City. The attenuation data presented for this earthquake would be representative of what could happen during a future earthquake of comparable magnitude in Gujarat.

Conclusions

The Kutch earthquake was a disaster affecting a large region of India. For proper engineering understanding of the phenomenon and to forecast the future hazard in the region, one needs strong motion records in the epicentral tract. In the absence of such instrumental data, the next best approaches for finding near source ground motion have been highlighted in this paper. Estimates based on analytical methods, as well as on field investigations are obtained and compared with PGA values back calculated from SRR instruments. A source mechanism model based on teleseismic data is used to obtain near source ground displacement time histories of an eight-layered regional model. PGA contours obtained analytically can be directly used to understand the pattern of damages and also the behavior of structures which did not

suffer appreciable damage during the main event. The attenuation data obtained for the earthquake forms valuable information for working out a rational attenuation formula for Peninsular India (IYENGAR and RAGHUKANTH, 2004). The analytical approach and further favorable comparison with observed PGA values, highlights the importance of adopting such methodology on a large scale for delineating the seismic hazard to Indian cities such as Delhi, Agra, Guwahati and Mumbai located near active faults.

Acknowledgements

REFERENCES

AMBRASEYS, N.N. (1974), *The correlation of intensity with ground motions*. In Advancements in Engineering Seismology in Europe, Trieste.

ARCHULETA, R.J. *et al.* (2003), *Finite-fault site-specific acceleration time histories that include nonlinear soil response*, Phys. Earth Planet Int. *137*(1–4), 153–181.

BERESNEV, I. and ATKINSON, G.M. (1997), *Modeling finite fault radiation from the wn spectrum*, Bull. Seismol. Soc. Am. *87*, 67–84.

BOORE, D.M. (1983), *Stochastic simulation of high frequency ground motions based on seismological models of the radiated spectra*, Bull. Seismol. Soc. Am. *73*, 1865–1894.

BOUCHON, M. (1981), *A simple method to calculate Green's functions for elastic layered media*, Bull. Seismol. Soc. Am. *71*, 959–971.

BSSC (2001), *NEHRP recommended provisions for seismic regulations for new buildings and other structures 2000 edition,Part 1: Provisions*, prepared by the Building Seismic Safety Council for the Federal Emergency Management Agency (Report No FEMA 368), Washington, D.C., USA.

CRAMER, C.H. and KUMAR, A. (2003), *2001 Bhuj, India earthquake engineering seismoscope recordings and eastern north America ground-motion attenuation relations*, Bull. Seismol. Soc. Am. *93*, 390–394.

DEPT. OF EARTHQUAKE ENGINEERING (2001). *Strong motion data from Kutch earthquake of January 26, 2001*, Report, Univ. of Roorkee, June 2001, pp. 1–27.

FRANKEL, A. (1995), *Simulating strong motion of large earthquakes using recordings of small earthquakes: The Loma Prieta mainshock as test case*, Bull. Seismol. Soc. Am. *85*, 1144–1160.

HARTZELL, S.H. (1978), *Earthquake aftershocks as Green's functions*, Geophys. Res. Lett. *5*, 1–4.

HISADA, Y. and MEGURO, K. (2001), *Estimation of macroseismic intensity*. In *A Comprehensive Survey of the 26 January 2001 Earthquake (M_w 7.7) in the State of Gujarat, India*, Research Report on Natural Disasters, Japan Ministry of Education, December 2001, pp. 56–63.

HUTCHINGS, L. (1994), *Kinematic earthquake models and synthesized ground motion using empirical Green's functions*, Bull. Seismol. Soc. Am. *84*, 1028–1050.

IMD (2002), *Bhuj Earthquake of January 26, 2001*, A consolidated document, Government of India, September 2002.

IYENGAR, R.N., MANOHAR, C.S., and JAISWAL, O.R. (1994), *Field investigation of the 30th September Maharashtra earthquake*, Current Science *67*(5), 368–379.

IYENGAR, R.N. *et al.* (2001), *Field investigation of the Kutch earthquake*, Unpublished Report. Dept. of Civil Eng., Ind. Inst. of Science, Bangalore.

IYENGAR, R.N. and RAGHUKANTH, S.T.G. (2003), *Attenuation of strong ground motion and site specific seismicity in Peninsular India*, Proc. of National Seminar on Seismic Design of Nuclear Power Plants, 21–22 February 2003, SERC Chennai, Allied Publ. Pvt. Ltd. N. Delhi, 269–291.

IYENGAR, R.N. and RAGHUKANTH, S.T.G. (2004), *Attenuation of strong ground motion in Peninsular India*, Seismol. Res. Lett. *79* (5), 530–540.

KANAMORI, H. and ANDERSON, D.L. (1975), *Theoretical basis of some empirical relations in seismology*, Bull. Seismol. Soc. Am. *65*, 1073–1095.

MORI, J. (2001), *Slip distribution of mainshock*. In *A Comprehensive Survey of the 26 January 2001 Earthquake (M_w 7.7) in the State of Gujarat, India*, Research Report on Natural Disasters, Japan Ministry of Education, December 2001, pp. 41–45.

NAKATA, T. *et al.* (2001), *Surface deformation around Budharmora*. In *A Comprehensive Survey of the 26 January 2001 Earthquake (M_w 7.7) in the State of Gujarat, India*, Research Report on Natural Disasters, Japan Ministry of Education, December 2001, pp. 56–63.

NEGISHI, H. *et al.* (2001), *Aftershocks and slip distribution of mainshock*. In *A Comprehensive Survey of the 26 January 2001 Earthquake (M_w 7.7) in the State of Gujarat, India*, Research Report on Natural Disasters, Japan Ministry of Education, December 2001, pp. 33–45.

PITARKA, A. *et al.* (2000), *Simulation of near-fault strong ground motion using hybrid Green's function*, Bull. Seismol. Soc. Am. *90*(3), 566–586.

RAJENDRAN, K. *et al.* (2001), *The 2001 Kutch (Bhuj) Earthquake: Coseismic surface features and their significance*, Current Science *80*(11), 1397–1405.

SINGH, S.K. *et al.* (2003), *Estimation of ground motion for Bhuj (26th January 2001. $M_W = 7.6$) and for future earthquakes in India*, Bull. Seismol. Soc. Am. *93*(1), 353–370.

THEOHARIS, A.P. and DEODATIS, G. (1994), *Seismic ground motion in a layered half-space due to a Haskell-type source. I: Theory*, Soil Dyn. Earthq. Engin. *13*(4), 281–292.

TRIFUNAC, M.D. and BRADY, A.G. (1975), *On the correlation of seismic intensity scales with the peaks of recorded strong ground motion*, Bull. Seismol. Soc. Am. *65*(1), 139–162.

WALD, D.J. *et al.* (1999), *Relationships between peak ground acceleration, peak ground velocity, and modified Mercalli intensity in California*, Earthquake Spectra *15*(3), 557–564.

To access this journal online:
http://www.birkhauser.ch